sustainability

MDPI

Article

Decadal Variation of Polycyclic Aromatic Hydrocarbons (PAHs) in an Area Contaminated by Coal Gangue Dump: Emphasis on Concentration, Profile, Source and Carcinogenic Risk

Yanli Yang [1,2,3], Minmin Zhang [1,2,*], Qiaojing Zhao [3], Balaji Panchal [3], Jinxi Wang [2,3], Kai Bian [3] and Yuzhuang Sun [3]

[1] School of Water Conservancy and Hydroelectric Power, Hebei University of Engineering, Handan 056038, China
[2] Key Laboratory of Resource Exploration Research of Hebei Province, Hebei University of Engineering, Handan 056038, China
[3] School of Earth Science and Engineering, Hebei University of Engineering, Handan 056038, China
* Correspondence: huezhangmm@126.com

Abstract: Polycyclic aromatic hydrocarbons (PAHs) are recognized as carcinogens that pose a severe threat to human health. Research on the temporal variation of PAHs was confined to monthly and seasonal investigations, and a longer timescale study remained inadequate until recently. Therefore, this study focuses on the decadal variation of PAHs in environmental media contaminated by a coal gangue dump in the Jiulong Coal Mine, Fengfeng, China. The results show that the total concentrations of PAHs have sharply declined compared to the past. The result of the paired-sample *t*-test indicates that several individual PAHs have obviously changed in concentration with statistical significance ($p < 0.05$). Moreover, proportions of medium-molecule weight PAHs increase with statistical significance ($p < 0.01$) when compared to the past. Various diagnostic ratios suggest that PAHs in previous samples are mainly derived from weathering products of coal gangue and vehicle exhaust, while PAHs in the present samples are dominated by those originating from pyrogenic sources. Calculation of incremental lifetime cancer risks (ILCRs) indicates high carcinogenic risk despite a considerable decrease in ILCR values by 2 to 3 orders of magnitude. It shows that recent measurements conducted by the local government do weaken the contamination of coal gangue dumps, but more attention to pyrogenic PAHs is necessary.

Keywords: polycyclic aromatic hydrocarbons; coal gangue dump; source apportionment; carcinogenic risk; decadal variation

check for updates

Citation: Yang, Y.; Zhang, M.; Zhao, Q.; Panchal, B.; Wang, J.; Bian, K.; Sun, Y. Decadal Variation of Polycyclic Aromatic Hydrocarbons (PAHs) in an Area Contaminated by Coal Gangue Dump: Emphasis on Concentration, Profile, Source and Carcinogenic Risk. *Sustainability* **2022**, *14*, 14371. https://doi.org/10.3390/su142114371

Academic Editors: Song Cui and Lihui An

Received: 9 September 2022
Accepted: 30 October 2022
Published: 2 November 2022

Publisher's Note: MDPI stays neutral with regard to jurisdictional claims in published maps and institutional affiliations.

Copyright: © 2022 by the authors. Licensee MDPI, Basel, Switzerland. This article is an open access article distributed under the terms and conditions of the Creative Commons Attribution (CC BY) license (https://creativecommons.org/licenses/by/4.0/).

1. Introduction

Polycyclic aromatic hydrocarbons are a group of persistent organic pollutants (POPs) that have two or more fused aromatic rings in diverse structural configurations [1,2]. It is well established that pyrolysis is the primary source of PAHs in environmental media, which includes vehicle exhaust, industrial emissions, and household heating. Those processes involving incomplete combustion of gasoline, diesel, coal and other solid biomass that could mainly generate medium and heavy molecule weight PAHs containing more than three benzene rings [3–5]. Petrogenic PAHs (2 to 3 benzene rings) are mainly derived from natural sources, such as coals and crude oil [3], as well as from the products of incomplete combustion at low temperature [6]. The aforementioned two sources are frequently involved in the source apportionment of PAHs in a number of previous studies [7–12]. In addition, biological sources of PAHs are identified, which can be formed in the processes of degradation of vegetative matter or synthesized by certain bacteria and plants [13]. On account of their various sources, as well as their properties of lipophilicity, hydrophobicity and recalcitrance, PAHs can be detected in soil, water and air and thus are recognized as ubiquitous contaminants in multiple environmental media [14].

Once PAHs are released from their sources into the environment, two major driving factors in the process of their migration can be identified: air and water. In the atmosphere, PAHs are chiefly combined with particulate materials and can transfer in the gaseous phase [15]. The formation processes of atmospheric PAHs are those initially forming gaseous PAHs that can be adsorbed on the particles by condensation during cooling after the emission, while those PAHs with high volatility would disengage from particulate incorporation and then remain in the gas phase in the atmosphere [16]. The transportation and fate of atmospheric PAHs are considerably controlled by the properties and behaviors of the carrier particulate matter, as well as meteorological conditions [17]. When PAHs enter the ground through dry or wet deposition, their transportation is dominated by weathering solutions and runoff. Not only can PAHs be desorbed from the surface of their previous adsorptive particulates and then dissolved in the solution, but they can also migrate as adsorbents in the form of a solid phase [18,19]. These processes are highly dependent on the solubility and octanol/water partition coefficient (namely K_{ow}) of certain PAHs. Through the processes of migration and precipitation, PAHs can be dispersed and accumulated in environmental media, ultimately inducing contamination. It has been reported that soil performs as the paramount and ultimate sink for PAHs [20].

PAHs have provoked extensive concerns owing to their pernicious characteristics of carcinogenicity, teratogenesis and mutagenesis; some of them have been classified as Class-I human carcinogen by IARC [21]. A large number of epidemiological investigations have indicated that high doses of environmental and occupational exposure to PAHs can induce various cancers, including bladder, lung, kidney, larynx, esophageal and skin carcinoma [22]. Therefore, a total of sixteen species of PAHs were classified as priority-controlled pollutants by the United States Environmental Protection Agency (USEPA) [23]. Among them, seven species of PAHs were further considered as priorities on account of their stronger threat to human health [24].

In view of their persistence in multiple environmental media, as well as their threat to human health, a large number of studies on PAHs have been conducted worldwide for a long time, of which purposes mainly focus on concentrations, profiles, distribution patterns, sources and spatio-temporal variations of PAHs in various environmental media including soil, sediment, river, lake, ocean, dust fall and atmospheric particulates [25–39]. Nonetheless, those studies in regard to the temporal variation of PAHs are mostly restricted to annual or seasonal changes in PAH concentrations. For example, Zheng et al. [30] researched seasonal differences of PM_{10}-PAHs in Huainan city in China, and their results indicated significant differences in total PAH concentrations between summer and winter, spring and summer and autumn and winter. Rekefu et al. [31] researched monthly variation of PAH concentration in $PM_{2.5}$ and $PM_{2.5–10}$ collected in Urumqi in 2011. They found that the highest concentration occurred in winter and the lowest in summer, which was mainly induced by local coal combustion. De Nicola et al. [32] bio-monitored PAH pollution in air in Naples, Italy by measuring the concentration of PAHs in leaves of a Mediterranean oak. They found a temporal trend that total PAH concentrations in leaves collected in winter were two times higher than those collected in other seasons. Brachtl et al. [33] focused on hourly variation of PAH concentrations at two near-roadway sites in Quito, Ecuador and found that daily maximum PAH concentrations occurred at the interval of morning traffic peak (6:00 to 8:00 a.m.) because of the surge of vehicle exhaust. Cheng et al. [34] observed seasonal variations in PAH concentrations and fluxes in atmospheric deposition in Shanghai City and found that the average concentration was highest in June and lowest in November during the sampling period, while the fluxes were higher in spring and winter than in summer and autumn. Research on the temporal variation of PAHs at a longer time scale still remains deficient until now.

The overarching aim of this study was to explore the temporal variation of PAHs on a long-term time scale by identifying the presence of well-defined differentiation in terms of concentrations and sources between the previous and present samples collected from a coal gangue dump and its vicinity. In addition, variation in carcinogenic risks induced by

PAHs within an interval of ten years was also unveiled. This paper would facilitate insight into a significant replacement of PAH sources that play the most important role in organic contamination. It is also beneficial to understand long-term variation and geochemical behavior of PAHs under a supergene environment and to provide scientific guidance for proactive prevention of PAH pollution.

2. Materials and Methods

2.1. Study Area

The coal gangue dump of Jiulong Coal Mine (36.435086 N, 114.264636 E) (Figure 1) was selected as the object of this study because it performs a source that continuously releases PAHs into the environment, and it was once investigated by our research team to explore the organic contamination of the Fengfeng Mining District. Previous samples included coal gangue, surface soil, sediment and background sample, of which sites were designed to be dispersed from north to south with increasing distance from the coal gangue dump. Jiulong Coal Mine is located in the southwest of Handan City. It is characterized by a rhombus distribution pattern in the eastern wing of Gushan Anticline, with an area of 20.2 km^2. The Jiulong Coal Mine was built in 1975 and completed in 1980. Its designed production capacity was 1.2 million tons/year while the actual production capacity was maintained at the level of 1.5 million tons/year. There is a thermal power plant and a washery in the Jiulong Coal Mine. Nos. $4^{\#}$, $6^{\#}$, $8^{\#}$ and $9^{\#}$ coal seams in Taiyuan Formation are the primary mineable coal seam of the Jiulong Coal Mine. Solid wastes produced in the process of coal mining were transported by an electric conveyor belt and stacked on the ground, forming a coal gangue dump with a diameter of more than 300 m and a height of approximately 30 m. The study area has a semi-arid continental monsoon climate, with an obvious difference in seasonal variation. The annual temperature and the annual average sunshine duration are 13.5 °C and 2357 h, respectively. Precipitation shows inhomogeneity in both spatial and temporal distribution, with an average annual precipitation of 545.8 mm.

2.2. Sampling Campaign

The coal gangue dump of the Jiulong Coal Mine was selected as the starting point of the sampling campaign due to its role as a point pollution source of PAHs in the surroundings. All sampling sites in this study were planned in strict accordance with the sites of our previous study [35]. The soil sample collection procedure followed the Chinese national standard GB/T 36197-2018 and Chinese industry standard DZ/T 0258-2014. A total of eleven samples were collected from the coal gangue dump of Jiulong Coal Mine and its vicinity. The coal gangue sample (JL1) was picked at the top of the gangue dump, where the fresh coal gangue was stacked. In terms of surface soil samples (JL2–JL7), plant debris, rocks and waste were discarded before the collection, and 3–15 cm depth surface soil was collected by using a stainless steel shovel and subsequently sealed in glass jars. In addition, four additional samples (BS, B6, B8 and B40) collected from the sediments of the Fuyang River were added in this study as a supplement to background information of PAHs. All samples were transported to the laboratory as soon as possible for the next processing. The sampling campaign was performed in November 2019. The data representative of PAH levels ten years ago, which is available in Sun et al. [35], is employed in this study for comparison.

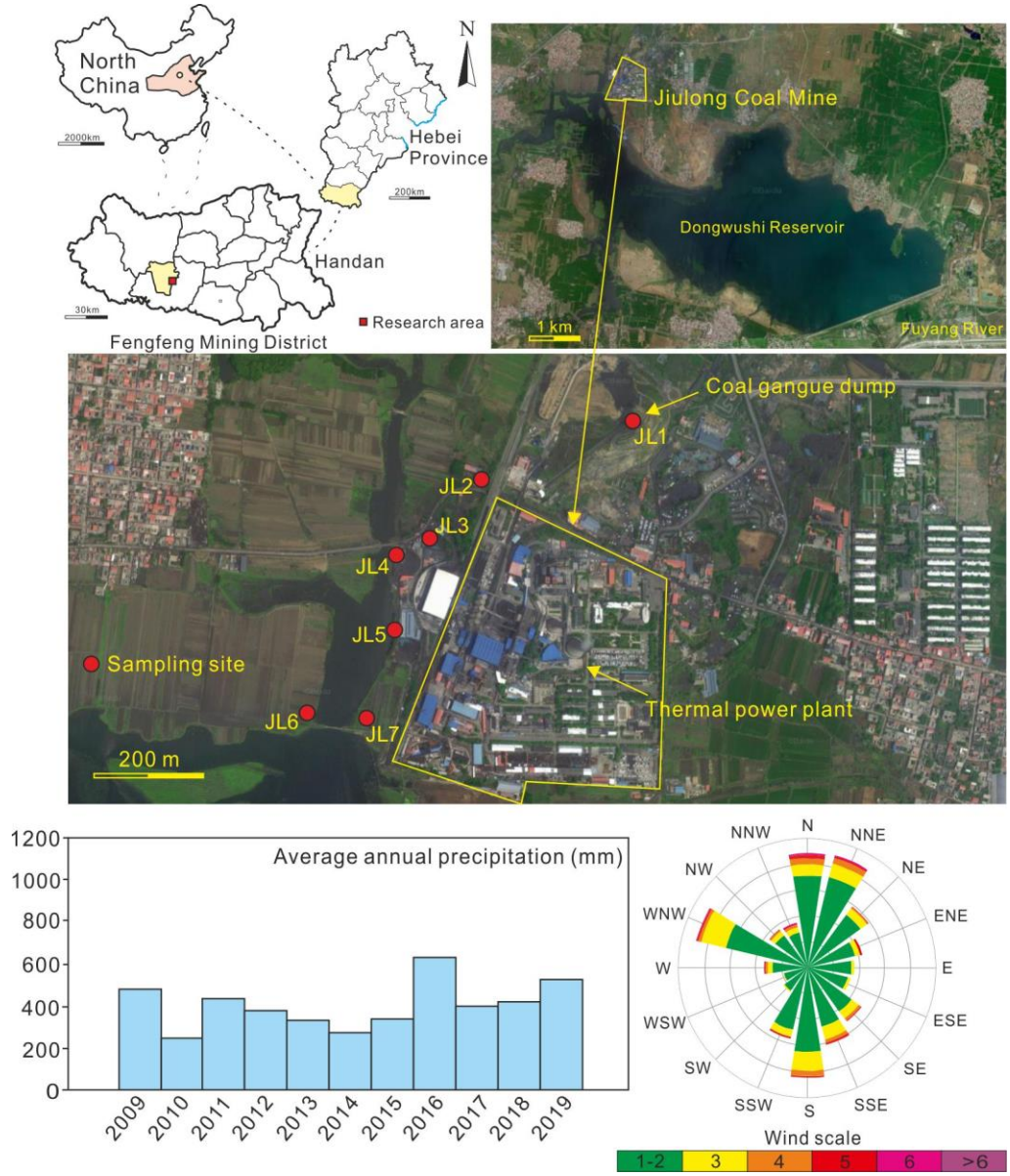

Figure 1. Location of study area and sampling sites with average annual precipitation and flattened windrose of study area in the period from 2009 to 2019.

2.3. Analytical Methods

The coal gangue sample was washed with ultra-pure water, then, together with surface soil and sediment samples, was air-dried at room temperature. After pulverization in the agate mortar, all samples were sieved with a 200-mesh sieve. An approximate 5 g sample (accurate to 0.0001 g) was weighed and transported into a 100 mL flask with a certain volume of surrogate standards spiking solution, including naphthalene D-18, acenaphthene D-10, phenanthrene D-10, chrysene D-12 and perylene D-12. The sample was soaked with 100 mL of mixed solvent composed of hexane and acetone (1:1, *v*:*v*) overnight, and then Soxhlet extracted for 24 h. After that, the solvent was exchanged into hexane. The rotary evaporator was used to reduce the volume of solvent to 5 mL, and a gentle N_2 stream was used to adjust the final volume to 2 mL. The extract was eluted by a 50 mL mixture of dichloromethane and hexane (1:1, *v*:*v*) through a column chromatography (300 mm × 19 mm i.d.) that was filled with 12 cm aluminum oxide, 12 cm silica gel and 1 cm anhydrous sodium sulfate in sequence. Aluminum oxide and silica gel were deactivated with 5% and 1% ultra-pure water, respectively. After being rinsed with

hexane, the elute of the PAH fraction was transferred into a Kuderna-Danish concentrator and evaporated to 1 mL by a gentle N_2 stream. A certain volume (1–50 µL) of squalane was spiked into the solution as an internal standard for quantitation.

A total of sixteen species of individual PAHs that were classified as priority-controlled pollutants by USEPA were quantified by a gas chromatograph coupled with a mass spectrometer (GC-MS) (Agilent 7890B-5977A MSD, Waltham, MA, USA) with a HP-5MS UI (30 m × 0.25 mm × 0.25 µm). Those sixteen individual PAHs contain naphthalane (Nap), acenaphthene (Ace), acenaphthylene (Acy), fluorene (Fl), phenanthrene (Phe), anthrancene (Ant), fluoranthene (Flu), pyrene (Pyr), benzo[a]anthracene (BaA), chrysene (Chr), benzo[b]fluoranthene (BbF), benzo[k]fluoranthene (BkF), benzo[a]pyrene (BaP), dibenzo[a,h]anthracene (DahA), benzo[g,h,i]perylene (BghiP) and indeno [1 2 3-c,d]pyrene (IcdP). The GC-MS was set to the "electron impact ionization" mode with a voltage of 70 eV. The temperatures of the injector, ion source and quadrupole were set to 295, 300, and 180 °C, respectively. The oven temperature procedure was set as follows: held at 60 °C for 5 min, and raised to 300 °C at a rate of 4 °C/min, then maintained for 15 min. 1 µL of samples were injected by autosampler in a "splitless" way. Helium was used as the carrier gas. To guarantee the accuracy of the test results, blank samples and replications were employed, and all samples were scanned in triplicate. The recoveries of spiked surrogate standards varied from 92% to 109%, with an average of 103%.

2.4. Carcinogenic Risk Assessment

To ensure the consistency of data, a standard model of incremental lifetime cancer risks (ILCRs) proposed by the USEPA [36] was used to evaluate carcinogenic risks induced by PAHs in the present samples. Carcinogenic risks through three exposure pathways, ingestion, inhalation and dermal contact, were quantitatively calculated in this study. Specific calculating methodologies are available in the Supplementary Materials and our previous study [37].

3. Results and Discussion

3.1. Concentrations and Profile of Present PAHs

The concentrations of PAHs measured in this study are listed in Table 1. The concentrations of $\sum PAH_{16}$ in soil and sediment samples vary from 43.94 to 3193 ng/g, with the mean and median of 825.0 ng/g and 482.1 ng/g respectively, while $\sum PAH_{16}$ concentration in coal gangue sample is 4483 ng/g. An evident trend that $\sum PAH_{16}$ concentrations decrease with the increase of distance between the sampling site and coal gangue dump is observed, which can be verified by a significantly negative Spearman's correlation between $\sum PAH_{16}$ concentration and the distance ($r = -0.818$ **, $p < 0.01$) (Table S3). It might be inferred that the coal gangue dump remains a source that continuously releases PAHs into nearby environmental media. Compared with other regions contaminated by coal mine, such as Huainan City, China [38] with $\sum PAH_{16}$ in surface soils of 109.9 to 1105 ng/g with an average of 528.1 ng/g, Tiefa Mining District, China [39] with $\sum PAH_{16}$ in soil of 5.1 to 5642.3 ng/g and $\sum PAH_{16}$ in coal gangue samples of 1678.2 to 3534.9 ng/g, and Tashkent, Uzbekistan [40] with $\sum PAH_{16}$ in soil of 70 to 4230 ng/g with an average of 1075 ng/g, study area shows a moderate level of PAH concentrations in environmental media. When compared with the average concentration of $\sum PAH_{16}$ (257.9 ng/g) in agricultural soils in eastern China [41], the study area showed a degree of PAH contamination. In terms of the samples representing the background value of PAH concentration in the research area, a considerable decline in PAH concentration, especially in B40, can be identified when compared to the samples that were closer to the coal gangue dump. The sampling site of B40 is far from the coal gangue dump, where agricultural soil barely suffered from organic contamination. By comparison, Ace, Fl, IcdP, DahA and BghiP in background samples show the most evident decline in the aspect of individual PAHs. The first two may originate from petrogenic sources (i.e., coal gangue) and the others may be products of vehicle exhaust. It can be consequently inferred that PAH composition in soils near the coal

gangue dump is influenced by a combination of petrogenic and pyrogenic input. Specific source apportionments for PAHs will be discussed in the next section.

Table 1. Concentrations [a] and compositional profile of PAHs in the present samples.

	JL1	JL2	JL3	JL4	JL5	JL6	JL7	B6	B8	B40	BS
Nap	117	1.20	44.5	7.56	7.59	0.39	0.94	BDL	BDL	BDL	0.08
Acy	10.9	0.00	0.00	6.08	1.51	1.32	0.29	BDL	BDL	BDL	BDL
Ace	247	45.7	133	25.9	53.2	4.92	2.86	5.77	13.5	0.11	2.63
Fl	558	77.5	254	24.2	62.4	11.9	8.14	12.5	19.1	0.00	9.06
Phe	1280	589	1202	143	293	67.1	25.8	84.7	34.4	8.39	61.9
Ant	84.3	48.2	109	4.49	23.8	12.7	3.09	9.41	3.58	0.91	3.14
Flu	256	143	299	43.0	109	33.9	26.1	93.0	28.6	6.06	45.1
Pyr	255	146	248	49.6	88.5	29.7	24.2	76.7	25.1	5.87	34.6
BaA	46.0	26.1	39.6	9.36	44.0	6.66	9.48	25.4	10.5	4.68	11.0
Chr	1057	314	538	45.5	249	53.0	16.1	44.9	92.3	4.88	34.12
BbF	112	78.0	72.3	12.5	49.8	32.3	11.4	18.7	21.8	3.99	23.1
BkF	290	91.4	127	5.78	57.6	22.3	2.73	11.0	14.5	3.78	39.7
BaP	56.8	18.5	18.6	8.30	17.0	10.1	2.99	7.05	7.92	5.27	11.9
IcdP	9.81	32.4	23.4	15.6	14.3	10.6	13.0	25.4	22.6	BDL	2.72
DahA	21.7	36.1	46.6	35.5	12.3	9.07	15.0	39.7	80.3	BDL	2.88
BghiP	81.0	20.4	37.4	63.5	32.2	7.89	26.4	28.0	85.3	BDL	5.76
$\sum PAH_{16}$	4483	1667	3193	500	1115	314	189	482	459	43.9	288
LMW-PAHs	51.24%	45.68%	54.59%	42.26%	39.62%	31.34%	21.81%	23.30%	15.37%	21.40%	26.69%
MMW-PAHs	36.00%	37.72%	35.22%	29.49%	43.94%	39.25%	40.25%	49.77%	34.05%	48.92%	43.40%
HMW-PAHs	12.76%	16.60%	10.19%	28.25%	16.44%	29.41%	37.95%	26.92%	50.59%	29.67%	29.90%
Distance [b]	0	150	320	570	930	1360	1330	6000	8000	40,000	1300

[a] The unit of individual PAHs and total PAH concentrations is ng/g. [b] represents the distance between respective sampling site and coal gangue dump (unit: m).

The specific proportion of PAHs is also listed in Table 1. Coal gangue is composed mainly of light molecule weight PAHs (LMW-PAHs, containing 2–3 aromatic rings) and accessorily medium molecule weight PAHs (MMW-PAHs, containing 4 aromatic rings) and heavy molecule weight PAHs (HMW-PAHs, containing 5–6 aromatic rings) in sequence (51.24%, 36.00% and 12.76% respectively). In terms of soil and sediment samples, proportions of LMW PAHs trend to decrease with the increased distance between sampling sites and coal gangue dumps, resulting in a gradual rise in proportions of MMW-PAHs. MMW-PAHs started to overtake LMW-PAHs as the majority from the sampling site of JL5. Similarly, MMW-PAHs also serve a primary role in background samples. In general, average percentages of LMW-, MMW- and HMW-PAHs in soil and sediment samples are 39.22%, 37.65% and 23.14%, respectively, while those in background samples are 21.70%, 44.03% and 34.27%, respectively. It is reasonable to infer that, therefore, the IcdPut of LMW-PAHs in nearby environmental media is derived from the coal gangue dump, of which attenuated influence can be portrayed by the variation of PAH profile.

3.2. Comparison of PAH Concentrations and Profiles

To distinguish the potential differences between previous and present PAHs, a paired-sample *t*-test was employed in this study (Table 2). The result suggests that Ant, BaA, IcdP, DahA and BghiP are changed in different degrees with statistical significance ($p < 0.05$). As shown in Table 2, the *t* values of those individual PAHs are all less than zero, indicating an evident increase in their concentrations. According to the absolute values of lower limits of 95% confidence interval (95%CI), Ant shows supreme degree of the decrease, followed by BhgiP, BaA, DahA and IcdP in sequence. In spite of the fact that some individual PAHs such as Acy, Ace, Ant, BaA, BkF, IcdP, DahA and BghiP were below detective limit previously but can be detected presently, the result of paired-sample *t*-test suggests that there is no statistical significance in variations of those individual PAH concentrations and therefore the variation of $\sum PAH_{16}$ has no statistical significance as well, although the visual

difference appears to be obvious (Figure 2). Additionally, $\sum PAH_{16}$ concentration in the previous coal gangue sample is approximately two times higher than that in the present coal gangue sample (Table 2), which could be attributed to different characteristics (especially organic component) of coal gangue between the previous and present exploited horizons. Some researchers have reported that organic coal petrological composition is collectively determined by parent materials and the sedimentary environment [42,43]. Concentration and profile of PAHs in coal and gangue are generally related to coal rank (or metamorphic degree), as well as the content of inertinite. Another phenomenon is that $\sum PAH_{16}$ in JL3 is higher than JL2 in both previous and present samples, which is contradictory to the negative correlation between PAH concentration and distance from the sampling site to the coal gangue dump. Although the sampling site of JL2 is closer to the source, JL3 was collected from the sediment of runoff, where weathering products (clastic particles and solution) are accumulated much easier. The sampling site of JL3 was once adjacent to the water of Dongwushi reservoir for a long time, rather than away from the water body presently. Therefore, a large amount of weathering products containing high concentrations of PAHs in the sampling site of JL3 induced the phenomenon above. By comparison, the sampling site of JL2 is hard to perform as a sink of PAHs as that of JL3, resulting from the lower capacity to transfer PAHs on the ground than through the runoff.

Table 2. Results of paired-sample *t*-test.

PAHs	Paired Difference					*t*	Significance (Two-Tailed)
	Average	Standard Deviation	Standard Error	95% Confidence Interval			
				Lower Limit	Upper Limit		
Nap	137.3	210.1	79.42	−57.07	331.6	1.728	0.135
Acy	−2.871	4.126	1.560	−6.688	0.945	−1.841	0.115
Ace	−73.23	88.30	33.38	−154.9	8.442	−2.194	0.071
Fl	586.3	816.1	308.4	−168.5	1341	1.901	0.106
Phe	967.2	1421	536.9	−346.7	2281	1.801	0.122
Ant	−40.80	41.67	15.75	−79.33	−2.261	−2.590	**0.041**
Flu	92.86	123.1	46.52	−20.97	206.7	1.996	0.093
Pyr	385.6	576.8	218.0	−147.9	919.0	1.769	0.127
BaA	−25.89	17.48	6.606	−42.05	−9.722	−3.919	**0.008**
Chr	55.34	359.0	135.7	−276.7	387.4	0.408	0.698
BbF	546.0	726.3	274.5	−125.8	1218	1.989	0.094
BkF	−85.26	101.3	38.28	−178.9	8.417	−2.227	0.068
BaP	721.1	789.3	298.3	−8.842	1451	2.417	0.052
IcdP	−17.02	8.124	3.071	−24.53	−9.502	−5.541	**0.001**
DahA	−25.18	14.29	5.402	−38.40	−11.96	−4.661	**0.003**
BghiP	−38.40	25.44	9.615	−61.93	−14.87	−3.993	**0.007**
∑PAH16	3183	4440	1678	−923.3	7289	1.897	0.107
LMW-PAHs	0.034	0.093	0.035	−0.052	0.120	0.962	0.373
MMW-PAHs	−0.112	0.062	0.024	−0.169	−0.054	−4.743	**0.003**
HMW-PAHs	0.078	0.093	0.035	−0.008	0.164	2.212	0.069

Note: The items in bold represent the difference between previous and present samples with statistical significance ($p < 0.05$).

In terms of PAH profile, the result of the paired-sample *t*-test indicates that variation of proportion of MMW-PAHs shows a statistically significant increase (Table 2). For the paired-sample *t*-test, when Sig. < 0.05 (two-tailed), it means null hypothesis of the model is refused, suggesting that a statistically significant difference exists. In addition, when $t < 0$, it means the concentration of a certain item in the present sample increases when compared with the past; otherwise, it indicates a decline. Variation of PAH profile between previous and present samples is shown in Figure 3. Compared with the past, proportions of MMW-PAHs in the present coal gangue sample increase together with a decreasing proportion of HMW PAHs, while the proportion of LMW-PAHs remains unchanged. This

pattern of change is inherited by JL2, JL3 and JL5, which are within 1 km away from the coal gangue dump, while JL4 shows an almost identical profile of PAHs. The other pattern is identified in the rest of the samples that are further away from the coal gangue dump (JL6 and JL7), namely that proportions of MMW-PAHs increase in the present samples, which is accompanied by the decline of LMW-PAH proportions. These samples could be subject to the contamination of PAHs from other potential sources.

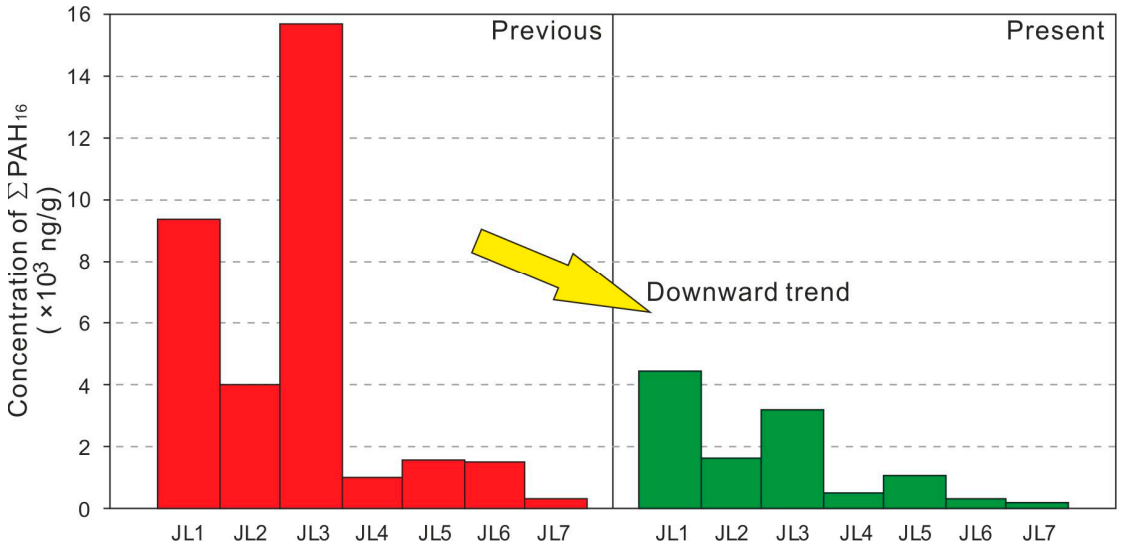

Figure 2. Variation of ∑PAH16 concentration.

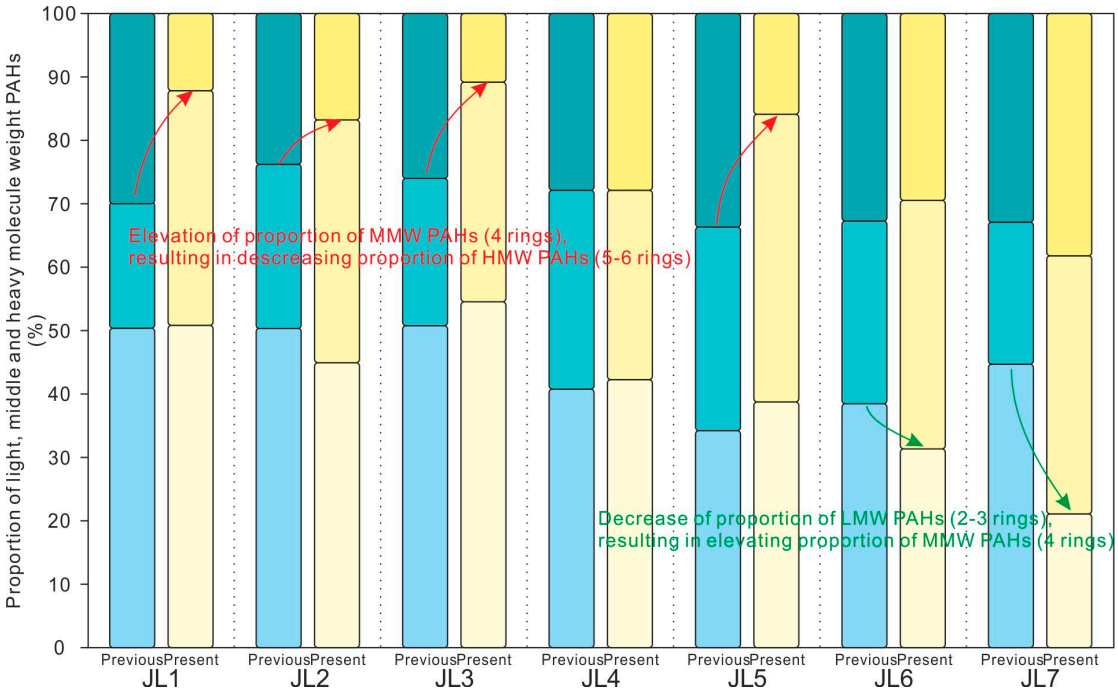

Figure 3. Variation of PAH profile (Rectangles of each column represent LMW-, MMW- and HMW-PAHs from the bottom to the top, respectively).

3.3. Comparison of Potential Sources of PAHs

Diagnostic ratios of PAHs are recognized as an effective and simple technique that has been widely used in source apportionment [44–47]. Considering that some individual PAHs were not detected in previous samples, a plot of PAHs' isomeric ratio Flu/(Flu + Pyr) vs. Flu/Pyr is employed in this study. An obvious distinction of distribution can be

identified between the previous and present samples (Figure 4). The ratios of Flu/Pyr in previous samples were all less than 1.0, indicating a petrogenic source [48]. For the ratios of Flu/(Flu + Pyr), JL3, JL5, JL6 and JL7 are less than 0.4, indicating petrogenic sources, while JL1, JL2 and JL4 are between 0.4 and 0.5, indicating liquid materials from pyrogenic sources such as incomplete combustion gasoline and diesel in vehicle engines. It is deduced from the previous samples that PAHs in samples collected from the sites near coal gangue dump are mainly derived from the weathering products of coal gangue, as well as vehicle exhaust released from the trucks for coal transportation, while PAHs in those collected from the sites far away from coal gangue dump originate exclusively from the weathering products of coal gangue. In terms of present samples, Flu/Pyr ratios of JL1, JL2 and JL4 are less than 1.0, indicating petrogenic source, while those of JL3, JL5, JL6 and JL7 are more than 1.0, indicating pyrogenic source. Similarly, JL1, JL2 and JL4 can be clustered into one group because their Flu/(Flu + Pyr) ratios range from 0.4 to 0.5, compared with JL3, JL5, JL6 and JL7, of which Flu/(Flu + Pyr) ratios are higher than 0.5. This suggests that PAHs in samples collected from sites far away from coal gangue dumps are dominated by solid materials of pyrogenic sources pertaining to the incomplete combustion of coal from nearby thermal power plant in the Jiulong Coal Mine. In addition, two other plots of PAHs isomeric ratios which are Flu/(Flu + Pyr) vs. Ant/(Ant + Phe) (Figure 5a) and IcdP/(IcdP + BghiP) vs. BaP/BghiP (Figure 5b), are employed in this study for cross calibration. According to the ratios of Ant/(Ant + Phe), JL6 and JL7 can be classified as combustion sources, while the rest of the samples can be classified as petrogenic sources [49]. The ratios of IcdP/(IcdP + BghiP) [50] suggest that JL1 is classified as a petrogenic source, which is in accordance with the reality that JL1 is a coal gangue sample. Moreover, the ratios of JL3, JL4, JL5 and JL7 range from 0.2 to 0.5, implying liquid materials of pyrogenic source, while those of JL2 and JL6 are more than 0.5, indicating solid materials of pyrogenic source. The ratios of BaP/BghiP show that JL1, JL2 and JL6 belong to traffic sources, while the rest can be classified as non-traffic sources.

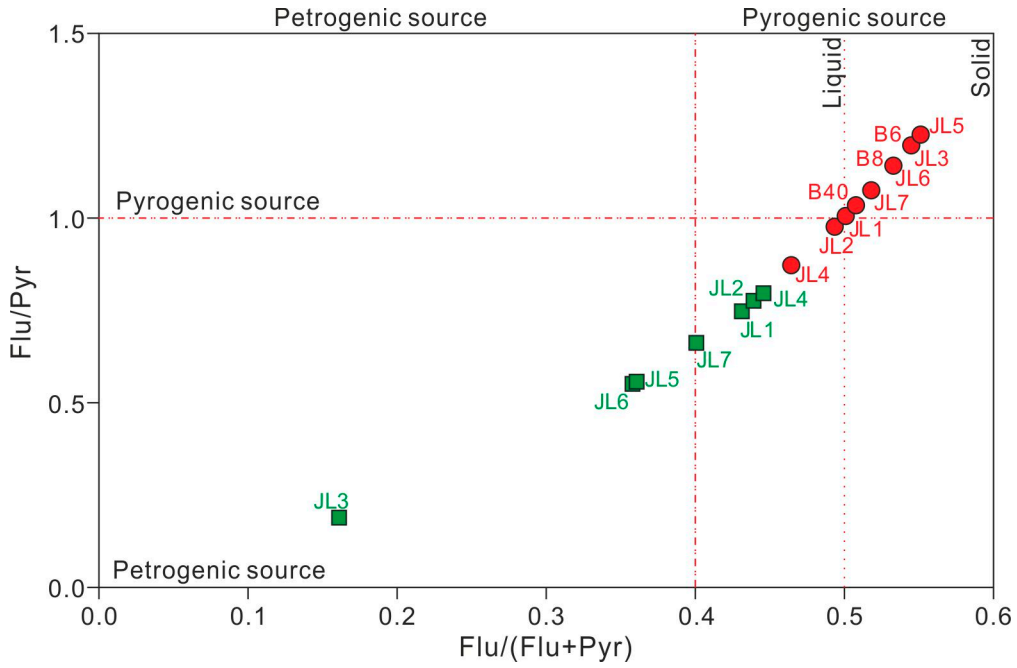

Figure 4. Plot of Flu/(Flu + Pyr) vs. Flu/Pyr (Green squares represent previous samples, while red circles represent present samples. The outliers are not displayed in the plot).

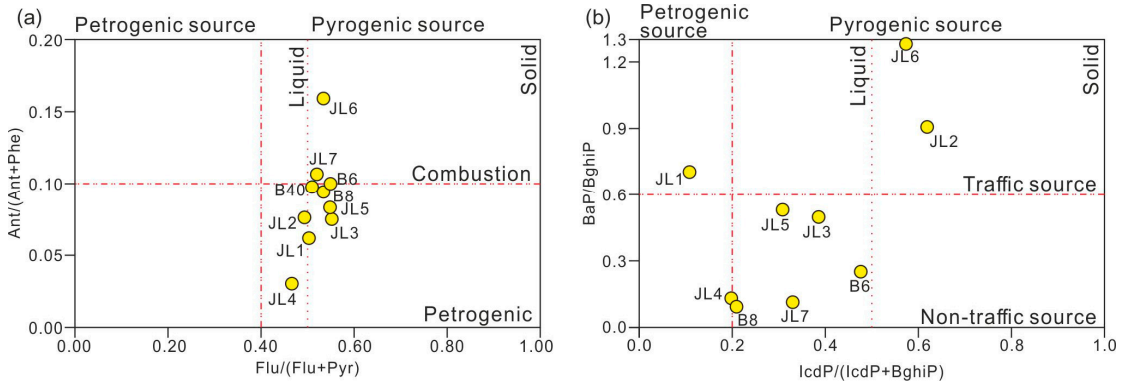

Figure 5. (**a**) Plots of Flu/(Flu + Pyr) vs. Ant/(Ant + Phe) and (**b**) IcdP/(IcdP + BghiP) vs. Bap/BghiP in the present samples (the outliers are not displayed in the plot).

In conclusion, PAHs in all previous samples are mainly derived from the weathering products of coal gangue (petrogenic), and vehicular exhaust induced by coal transportation (pyrogenic: liquid) also contributes a certain amount of PAHs in the samples collected from the vicinity of Jiulong Coal Mine. In contrast, the proportion of PAHs from incomplete combustion of liquid and solid materials (i.e., diesel, gasoline and coal) significantly rises in present samples, especially those far away from the coal gangue dump. Moreover, Spearman's correlation analysis (Table S3) shows that LMW-PAHs is negatively correlated with distance ($r = -0.918$ **, $p < 0.01$), indicating that LMW-PAHs originate from coal gangue and their concentrations decline sharply with increasing distance. It is reasonable to speculate that the present influencing scope of coal gangue dumps on PAHs has decreased considerably compared with the past. We found that almost all coal gangue dumps in the Fengfeng Mining District were covered by thick soils to prevent weathering of coal gangue during field investigation and sampling. The conclusion of source apportionment proves that effective measures of pollution management by local government lead to conspicuous decline of both PAH concentration and influencing scope of coal gangue dump. The degradation and transformation of PAHs that have already occurred in environmental media in supergene environments could be other reasons for the decline in PAH concentrations. Positive correlation between HMW-PAHs and distance ($r = 0.718$ *, $p < 0.05$) (Table S3) in combination with increasing proportion of MMW- and HMW-PAHs in present samples (Figure 3) indicate occurrence of pyrogenic PAHs in the samples away from coal gangue dump. Those PAHs generated in burning processes of coal, biomass, gasoline and diesel are no longer negligible components when compared with the past.

3.4. Comparison of Potential Carcinogenic Risks

The results of the ILCR calculations for PAHs in the present samples are listed in Table 3. The coal gangue sample shows the highest carcinogenic risks for all gender and age groups. For soil and sediments samples, total ILCR values for male adult, female adult, male child and female child vary from 7.54×10^{-5} to 9.09×10^{-4}, 7.83×10^{-5} to 9.45×10^{-4}, 4.07×10^{-5} to 4.91×10^{-4} and 3.93×10^{-5} to 4.74×10^{-4} respectively, with averages of 4.67×10^{-4}, 4.85×10^{-4}, 2.52×10^{-4} and 2.43×10^{-4} respectively. The order of total carcinogenic risks suffered by different groups is female adult > male adult > male child > female child. In terms of the exposure pathway, carcinogenic risks induced by ingestion and dermal contact are similar, both of which are four to five orders of magnitude higher than the risks resulting from inhalation. For gender groups, the three exposure pathways of male adults were merely less than those of female adults. In contrast, the three exposure pathways of male children slightly exceeded those of female children. An evident difference can be observed in respect to age groups; carcinogenic risks suffered by adults are approximately 1 to 3 times higher than those suffered by children. The USEPA [51] recommended a schedule that ILCRs < 1.00×10^{-6} indicate acceptable level and ILCRs in the range of 1.00×10^{-6} to 1.00×10^{-4} represent potential risk, while ILCRs > 1.00×10^{-4}

mean that considerable carcinogenic risks would be induced and prior attention should be paid immediately. It is clear that all the ILCR values exceed the permissible threshold (1.00×10^{-4}) (Figure 6), indicating high carcinogenic risks to local residents. As shown in Table 3, even the risk induced by individual exposure pathways, such as ingestion and dermal contact, can reach the permissible threshold by itself. Nonetheless, calculated ILCR values are possibly underestimated because the actual exposure frequency and duration for special occupational groups (e.g., farmer and miner) are likely higher than the parameters in ILCR calculations.

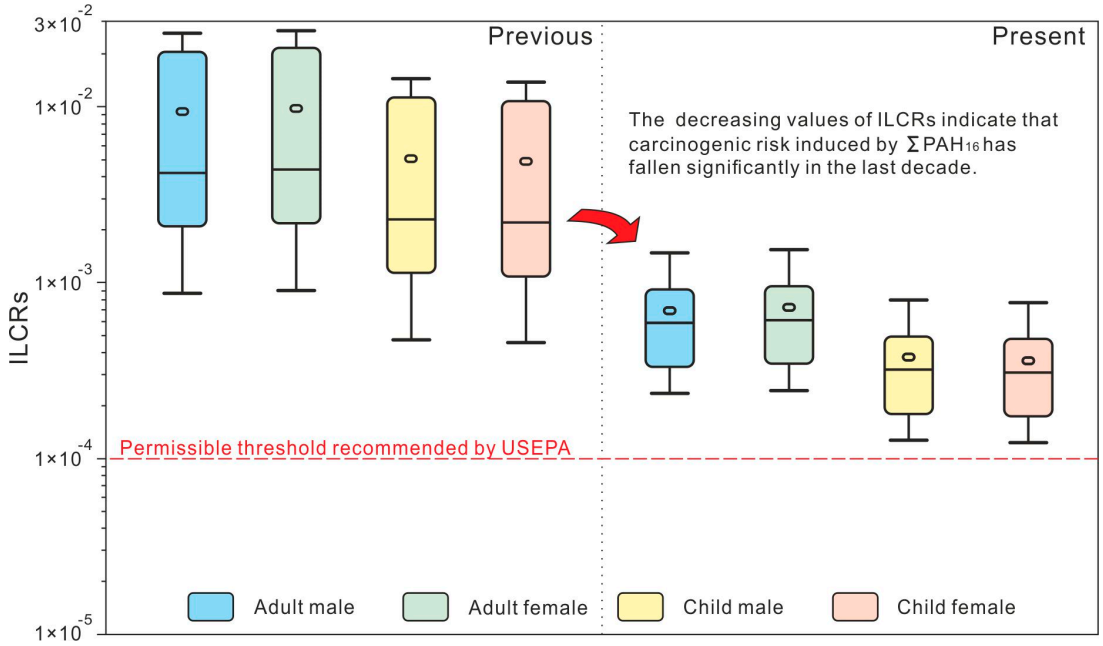

Figure 6. Variation of calculated values of ILCRs (three horizontal bars represent maximum, average and minimum from the top to the bottom, respectively). The upper and lower margins of the box represent the upper and lower quartiles, respectively. Ellipse in box represents median. The ILCR values of previous samples are available in Zhang et al. [40]).

Compared with the past, carcinogenic risks caused by the present samples show a marked decline by 1 to 2 orders of magnitude (Figure 6). Although $\sum PAH_{16}$ concentrations have fallen in the last decade (Table 1, Figure 2), their degree of decrease cannot match that of ILCRs. The latter is caused by the amplification effect of the toxic equivalent factors (TEFs) employed in ILCR calculations. Decreasing concentrations of BaP and BbF (their TEFs are 1.0 and 0.1, respectively) mainly facilitate a substantial decline of carcinogenic risks with average rates of 98.39% and 91.20%, respectively, despite slight elevations of concentrations of other individual PAHs with high TEFs values (TEFs = 0.1) (e.g., BaA, BkF, IcdP and DahA). Moreover, variations of PAHs with lower TEFs values (TEFs = 0.01 or 0.001) (e.g., Nap, Acy, Ace, Fl, Phe, Flu, Ant, Pyr, Chr and BghiP) are more difficult to influence the final result of ILCRs. Although the ILCR values have decreased considerably when compared with the past, carcinogenic risks remain severe, suggesting that proactive measurements are of the utmost requirement.

Table 3. Result of ILCR calculation for PAHs in present samples (unitless).

	Ingestion				Inhalation				Dermal Contact				Total Carcinogenic Risk			
	Adult		Child		Adult		Child		Adult		Child		Adult		Child	
	Male	Female	Male	Female	Male	Female	Male	Female	Male	Female	Male	Female	Male	Female	Male	Female
JL1	7.31×10^{-4}	7.60×10^{-4}	2.07×10^{-4}	2.00×10^{-4}	2.48×10^{-8}	2.58×10^{-8}	8.74×10^{-9}	8.44×10^{-9}	7.39×10^{-4}	7.68×10^{-4}	5.87×10^{-4}	5.67×10^{-4}	1.47×10^{-3}	1.53×10^{-3}	7.94×10^{-4}	7.67×10^{-4}
JL2	4.48×10^{-4}	4.66×10^{-4}	1.27×10^{-4}	1.22×10^{-4}	1.52×10^{-8}	1.58×10^{-8}	5.36×10^{-9}	5.18×10^{-9}	4.53×10^{-4}	4.71×10^{-4}	3.60×10^{-4}	3.48×10^{-4}	9.01×10^{-4}	9.37×10^{-4}	4.87×10^{-4}	4.70×10^{-4}
JL3	4.52×10^{-4}	$4.70 \times 10\text{-}4$	1.28×10^{-4}	1.24×10^{-4}	1.53×10^{-8}	1.59×10^{-8}	5.41×10^{-9}	5.22×10^{-9}	4.57×10^{-4}	4.75×10^{-4}	3.63×10^{-4}	3.51×10^{-4}	9.09×10^{-4}	9.45×10^{-4}	4.91×10^{-4}	4.74×10^{-4}
JL4	1.80×10^{-4}	1.87×10^{-4}	5.09×10^{-5}	4.92×10^{-5}	6.11×10^{-9}	6.35×10^{-9}	2.15×10^{-9}	2.08×10^{-9}	1.82×10^{-4}	1.89×10^{-4}	1.45×10^{-4}	1.40×10^{-4}	3.62×10^{-4}	3.76×10^{-4}	1.95×10^{-4}	1.89×10^{-4}
JL5	2.92×10^{-4}	3.03×10^{-4}	8.26×10^{-5}	7.98×10^{-5}	9.91×10^{-9}	1.03×10^{-8}	3.49×10^{-9}	3.37×10^{-9}	2.95×10^{-4}	3.07×10^{-4}	2.35×10^{-4}	2.26×10^{-4}	5.87×10^{-4}	6.10×10^{-4}	3.17×10^{-4}	3.06×10^{-4}
JL6	1.63×10^{-4}	1.69×10^{-4}	4.60×10^{-5}	4.44×10^{-5}	5.52×10^{-9}	5.74×10^{-9}	1.95×10^{-9}	1.88×10^{-9}	1.65×10^{-4}	1.71×10^{-4}	1.31×10^{-4}	1.26×10^{-4}	3.27×10^{-4}	3.40×10^{-4}	1.77×10^{-4}	1.71×10^{-4}
JL7	1.16×10^{-4}	1.21×10^{-4}	3.28×10^{-5}	3.17×10^{-5}	3.94×10^{-9}	4.09×10^{-9}	1.39×10^{-9}	1.34×10^{-9}	1.17×10^{-4}	1.22×10^{-4}	9.32×10^{-5}	8.99×10^{-5}	2.33×10^{-4}	2.42×10^{-4}	1.26×10^{-4}	1.22×10^{-4}
B6	2.45×10^{-4}	2.54×10^{-4}	6.92×10^{-5}	6.68×10^{-5}	8.30×10^{-9}	8.62×10^{-9}	2.92×10^{-9}	2.82×10^{-9}	2.47×10^{-4}	2.57×10^{-4}	1.96×10^{-4}	1.90×10^{-4}	4.92×10^{-4}	5.11×10^{-4}	2.66×10^{-4}	2.56×10^{-4}
B8	2.57×10^{-4}	2.67×10^{-4}	7.26×10^{-5}	7.01×10^{-5}	8.71×10^{-9}	9.05×10^{-9}	3.07×10^{-9}	2.96×10^{-9}	2.59×10^{-4}	2.70×10^{-4}	2.06×10^{-4}	1.99×10^{-4}	5.16×10^{-4}	5.36×10^{-4}	2.79×10^{-4}	2.69×10^{-4}
B40	3.75×10^{-5}	3.89×10^{-5}	1.06×10^{-5}	1.02×10^{-5}	1.27×10^{-9}	1.32×10^{-9}	4.48×10^{-10}	4.33×10^{-10}	3.79×10^{-5}	3.94×10^{-5}	3.01×10^{-5}	2.91×10^{-5}	7.54×10^{-5}	7.83×10^{-5}	4.07×10^{-5}	3.93×10^{-5}
BS	1.30×10^{-4}	1.35×10^{-4}	3.68×10^{-5}	3.55×10^{-5}	4.41×10^{-9}	4.59×10^{-9}	1.56×10^{-9}	1.50×10^{-9}	1.32×10^{-4}	1.37×10^{-4}	1.04×10^{-4}	1.01×10^{-4}	2.62×10^{-4}	2.72×10^{-4}	1.41×10^{-4}	1.36×10^{-4}

4. Conclusions

PAHs in multiple environmental media in the vicinity of the Jiulong Coal Mine were measured in this study. The results show that $\sum PAH_{16}$ concentration in coal gangue is 4483 ng/g, while that in soil and sediment samples ranges between 43.94 and 3193 ng/g with average and median of 825.0 and 482.1 ng/g respectively. An evident trend is that $\sum PAH_{16}$ concentration decreases with increasing distance between the sampling site and coal gangue dump. Similarly, the proportion of LMW-PAHs tended to decrease in the samples far away from the coal gangue dump, which was accompanied by a relative increase in the proportions of MMW- and HMW-PAHs.

Compared with the past (a decade ago), several individual PAH, such as Ant, BaA, IcdP, DahA and BghiP, show an obvious variation with statistical significance ($p < 0.05$) according to the result of the paired-sample *t*-test. In terms of variation of PAH profile, two patterns can be identified: one is increasing proportion of MMW-PAHs coupled with decreasing proportion of HMW-PAHs, and the other is increasing proportion of MMW-PAHs accompanied by decreasing proportion of LWM-PAHs.

The results of source apportionment indicate that PAHs in previous samples are mainly derived from the weathering products of coal gangue, and pyrogenic PAHs induced by vehicle exhaust also make a contribution. In contrast, PAHs in the present samples have shifted to be dominated by pyrogenic PAHs originating from incomplete combustion of coal, biomass, gasoline and diesel.

The calculated ILCR values of the present samples significantly decreased by 1 to 2 orders of magnitude when compared with the past. Nevertheless, there are also high carcinogenic risks suffered by local residents due to present ILCR values still exceeding the permissible threshold (1.0×10^{-4}) recommended by the USEPA.

This study portrays and discusses decadal variations in the concentration, profile, source and carcinogenic risk of PAHs in multiple environmental media in the vicinity of a coal gangue dump. It is obvious that measurements conducted by local governments have weakened the capacity of coal gangue dumps that generate PAH contamination in their surroundings. It remains unclear, however, whether the degradation and transformation of PAHs occur under supergene conditions. Thus, the geochemical behavior of PAHs as well as their potential derivatives in environmental media merit intensive study in the future.

Supplementary Materials: The following supporting information can be downloaded at https://www.mdpi.com/article/10.3390/su142114371/s1, Table S1: The toxic equivalent factors (TEFs) of 16 individual PAH; Table S2: Parameters chose for the calculation of ILCRs; Table S3: Matrix of Spearman's correlation analysis for present samples. References [36,37,52–59] are cited in Supplementary Materials.

Author Contributions: Y.Y. and Q.Z.: Methodology, investigation, formal analysis, writing, visualization; M.Z., B.P., J.W. and K.B.: Conceptualization, methodology; M.Z. and Y.S.: Review and editing; Y.S.: Funding acquisition, project administration and Supervision. All authors have read and agreed to the published version of the manuscript.

Funding: This work was supported by the Ecological Wisdom Mine Joint Fund of the Natural Science Foundation of Hebei Province, grant number D2020402013.

Institutional Review Board Statement: Not applicable.

Informed Consent Statement: Not applicable.

Data Availability Statement: The datasets of this study are available from the corresponding author on reasonable request.

Acknowledgments: The authors thank Jingsen Fan and Peng Qin for their help in the sampling campaign a decade ago. The authors also appreciate anonymous reviewers for their constructive comments that improved the quality of this manuscript.

Conflicts of Interest: The authors declare no conflict of interest.

References

1. Kaplan, B.O.; Litman, R. Polycyclic aromatic hydrocarbons in soils of a mountain valley: Correlation with highway traffic and cancer incidence. *Environ. Sci. Technol.* **1978**, *12*, 599. [CrossRef]
2. Lawal, A.T. Polycyclic aromatic Hydrocarbons. A review. *Cogent Environ. Sci.* **2017**, *3*, 1339841. [CrossRef]
3. Hindersmann, B.; Achten, C. Urban soils impacted by tailings from coal mining: PAH source identification by 59 PAHs, BPCA and alkylated PAHs. *Environ. Pollut.* **2018**, *242*, 1217–1225. [CrossRef]
4. Yunker, M.B.; Perreault, A.; Lowe, C.J. Source apportionment of elevated PAH concentrations in sediments near deep marine outfalls in Esquimalt and Victoria, BC, Canada: Is coal from an 1891 shipwreck the source? *Org. Geochem.* **2012**, *46*, 12–37. [CrossRef]
5. Zhang, Y.; Tao, S.; Shen, H.; Ma, J. Inhalation exposure to ambient polycyclic aromatic hydrocarbons and lung cancer risk of Chinese population. *Proc. Natl. Acad. Sci. USA* **2009**, *106*, 21063–21067. [CrossRef] [PubMed]
6. Menzie, C.A.; Potocki, B.B.; Santodonato, J. Exposure to carcinogenic PAHs in the environment. *Environ. Sci. Technol.* **1992**, *26*, 1278–1284. [CrossRef]
7. Cassin, D.; Dominik, J.; Botter, M.; Zonta, R. PAH and PCB contamination in the sediments of the Venice Lagoon (Italy) before the installation of the MOSE flood defence works. *Environ. Sci. Pollut. Res.* **2018**, *25*, 24951–24964. [CrossRef]
8. Ontiveros-Cuadras, J.F.; Ruiz-Fernández, A.C.; Sanchez-Cabeza, J.-A.; Sericano, J.; Pérez-Bernal, L.H.; Páez-Osuna, F.; Dunbar, R.B.; Mucciarone, D.A. Recent history of persistent organic pollutants (PAHs, PCBs, PBDEs) in sediments from a large tropical lake. *J. Hazard. Mater.* **2018**, *368*, 264–273. [CrossRef]
9. Sosa, D.; Hilber, I.; Faure, R.; Bartolomé, N.; Fonseca, O.; Keller, A.; Bucheli, T.D.; Escobar, A. Polycyclic aromatic hydrocarbons and polychlorinated biphenyls in urban and semi-urban soils of Havana, Cuba. *J. Soil Sediment.* **2019**, *19*, 1328–1341. [CrossRef]
10. Sun, Z.; Zhu, Y.; Zhuo, S.; Liu, W.; Zeng, E.Y.; Wang, X.; Xing, B.; Tao, S. Occurrence of nitro- and oxy-PAHs in agricultural soils in eastern China and excess lifetime cancer risks from human exposure through soil ingestion. *Environ. Int.* **2017**, *108*, 261–270. [CrossRef]
11. Yurdakul, S.; Çelik, I.; Çelen, M.; Öztürk, F.; Cetin, B. Levels, temporal/spatial variations and sources of PAHs and PCBs in soil of a highly industrialized area. *Atmos. Pollut. Res.* **2019**, *10*, 1227–1238. [CrossRef]
12. Zhen, Z.; Yin, Y.; Chen, K.; Zhen, X.; Zhang, X.; Jiang, H.; Wang, H.; Kuang, X.; Cui, Y.; Dai, M.; et al. Concentration and atmospheric transport of PM2.5-bound polycyclic aromatic hydrocarbons at Mount Tai, China. *Sci. Total Environ.* **2021**, *786*, 147513. [CrossRef] [PubMed]
13. Abdel-Shafy, H.I.; Mansour, M.S.M. A review on polycyclic aromatic hydrocarbons: Source, environmental impact, effect on human health and remediation. *Egypt. J. Petrol.* **2016**, *25*, 107–123. [CrossRef]
14. Baklanov, A.; Hänninen, O.; Slørdal, L.H.; Kukkonen, J.; Bjergene, N.; Fay, B.; Finardi, S.; Hoe, S.C.; Jantunen, M.; Karppinen, A.; et al. Integrated systems for forecasting urban meteorology, air pollution and population exposure. *Atmos. Chem. Phys.* **2007**, *7*, 855–874. [CrossRef]
15. Marty, J.C.; Tissier, M.J.; Saliot, A. Gaseous and particulate polycyclic aromatic hydrocarbons (PAH) from the marine atmosphere. *Atmos. Environ.* **1984**, *18*, 2183–2190. [CrossRef]
16. Broddin, G.; Cautreels, W.; Van Cauwenberghe, K. On the aliphatic and polyaromatic hydrocarbon levels in urban and background aerosols from Belgium and the Netherlands. *Atmos. Environ.* **1980**, *14*, 895–910. [CrossRef]
17. Baker, J.E.; Eisenreich, S.J. Concentration and fluxes of polycyclic aromatic hydrocarbons and polychlorinated biphenyls across air-water interface of Lake Superior. *Environ. Sci. Technol.* **1990**, *24*, 342–352. [CrossRef]
18. ATSDR. *Polycyclic Aromatic Hydrocarbons*; U.S. Public Health Statement: Atlanta, GA, USA, 1990.

19. Nguyen, T.N.T.; Park, M.-K.; Son, J.-M.; Choi, S.-D. Spatial distribution and temporal variation of polycyclic aromatic hydrocarbons in runoff and surface water. *Sci. Total Environ.* **2021**, *793*, 148339. [CrossRef]
20. Lemieux, C.L.; Long, A.S.; Lambert, I.B.; Lundstedt, S.; Tysklind, M.; White, P.A. Cancer risk assessment of polycyclic aromatic hydrocarbon contaminated soils determined using bioassay-derived levels of benzo[a]pyrene equivalents. *Environ. Sci. Technol.* **2015**, *49*, 1797–1805. [CrossRef]
21. Yun, Y.; Gao, R.; Yue, H.; Liu, X.; Li, G.; Sang, N. Polycyclic aromatic hydrocarbon (PAH)-containing soils from coal gangue stacking areas contribute to epithelial to mesenchymal transition (EMT) modulation on cancer cell metastasis. *Sci. Total Environ.* **2017**, *580*, 632–640. [CrossRef]
22. Boffetta, P.; Jourenkova, N.; Gustavsson, P. Cancer risk from occupational and environmental exposure to polycyclic aromatic hydrocarbons. *Cancer Cause. Control* **1997**, *8*, 444–472. [CrossRef] [PubMed]
23. Keith, L.H.; Telliard, W.A. Priority pollutants. I. A perspective view. *Environ. Sci. Technol.* **1973**, *13*, 416–423. [CrossRef]
24. Wołejko, E.; Wydro, U.; Jabłońska-Trypuć, A.; Butarewicz, A.; Łoboda, T. The effect of sewage sludge fertilization on the concentration of PAHs in urban soils. *Environ. Pollut.* **2018**, *232*, 347–357. [CrossRef] [PubMed]
25. Boll, E.S.; Christensen, J.H.; Holm, P.E. Quantification and source identification of polycyclic aromatic hydrocarbons in sediment, soil, and water spinach from Hanoi, Vietnam. *J. Environ. Monit.* **2008**, *10*, 261–269. [CrossRef] [PubMed]
26. Mukherjee, A.; Agrawal, M. World air particulate matter: Source, distribution and health effect. *Envion. Chem. Lett.* **2017**, *15*, 283–309. [CrossRef]
27. Ruiz-Fernández, A.C.; Ontiveros-Cuadras, J.F.; Sericano, J.L.; Sanchez-Cabeza, J.-A.; Kwong, L.L.W.; Dunbar, R.B.; Mucciarone, D.A.; Pérez-Bernal, L.H.; Páez-Osuna, F. Long-range atmospheric transport of persistent organic pollutants to remote lacustrine environments. *Sci. Total Environ.* **2014**, *493*, 505–520. [CrossRef]
28. Wnorowski, A.; Charland, J.P. Profiling quinones in ambient air samples collected from Athabasca region (Canada). *Chemosphere* **2017**, *189*, 55–66. [CrossRef]
29. Yang, J.; Sun, P.; Zhang, X.; Wei, X.-Y.; Huang, Y.-P.; Du, W.-N.; Qadeer, A.; Liu, M.; Huang, Y. Source apportionment of PAHs in roadside agricultural soils of a megacity using positive matrix factorization receptor model and compound-specific carbon isotope analysis. *J. Hazard. Mater.* **2021**, *403*, 123592. [CrossRef] [PubMed]
30. Zheng, L.; Ou, J.; Liu, M.; Chen, Y.; Tang, Q.; Hu, Y. Seasonal and spatial variations of PM_{10}-bounded PAHs in a coal mining city, China: Distribution, sources, and health risks. *Ecotoxicol. Environ. Safe.* **2019**, *169*, 470–478. [CrossRef]
31. Rekefu, S.; Talifu, D.; Gao, B.; Turap, Y.; Maihemuti, M.; Wang, X.; Abulizi, A. Polycyclic Aromatic Hydrocarbons in $PM_{2.5}$ and $PM_{2.5–10}$ in Urumqi, China: Temporal Variations, Health Risk, and Sources. *Atmosphere* **2018**, *9*, 412. [CrossRef]
32. De Nicola, F.; Maisto, G.; Prati, M.V.; Alfani, A. Temporal variations in PAH concentrations in Quercus ilex L. (holm oak) leaves in an urban area. *Chemosphere* **2005**, *61*, 432–440. [CrossRef] [PubMed]
33. Brachtl, M.V.; Durant, J.L.; Perez, C.P.; Oviedo, J.; Sempertegui, F.; Naumova, E.N.; Griffiths, J.K. Spatial and temporal variations and mobile source emissions of polycyclic aromatic hydrocarbons in Quito, Ecuador. *Environ. Pollut.* **2009**, *157*, 528–536. [CrossRef] [PubMed]
34. Cheng, C.; Bi, C.; Wang, D.; Yu, Z.; Chen, Z. Atmospheric deposition of polycyclic aromatic hydrocarbons (PAHs) in Shanghai: The spatio-temporal variation and source identification. *Front. Earth Sci.* **2018**, *1*, 63–71. [CrossRef]
35. Sun, Y.Z.; Fan, J.S.; Qin, P.; Niu, H.Y. Pollution extents of organic substances from a coal gangue dump of Jiulong Coal Mine, China. *Environ. Geochem. Health* **2009**, *31*, 81–89. [CrossRef]
36. USEPA. Exposure factors handbook. In *Final Report*, 2011st ed.; EPA/600/R-09/052F; Environmental Protection Agency: Washington, DC, USA, 2011.
37. Zhang, M.; Wang, J.; Zhao, Q.; Mishra, V.; Fan, J.; Sun, Y. Polycyclic aromatic hydrocarbons (PAHs) and esophageal carcinoma in Handan-Xingtai District, North China: A preliminary study based on cancer risk assessment. *Environ. Monit. Assess.* **2020**, *192*, 596. [CrossRef] [PubMed]
38. Zhang, J.; Liu, F.; Huang, H.; Wang, R.; Xu, B. Ocurrence, risk and influencing factors of polycyclic aromatic hydrocarbons in surface soils from a large-scale coal mine, Huainan, China. *Exotoxicol. Environ. Safe.* **2020**, *192*, 110269. [CrossRef]
39. Liu, J.; Liu, G.; Zhang, J.; Yin, H.; Wang, R. Occurrence and risk assessment of polycyclic aromatic hydrocarbons in soil from the Tiefa coal mine district, Liaoning, China. *J. Environ. Monit.* **2012**, *14*, 2634. [CrossRef]
40. Bandowe, B.A.M.; Shukurov, N.; Kersten, M.; Wilcke, W. Polycyclic aromatic hydrocarbons (PAHs) and their oxygen-containing derivatives (OPAHs) in soils from the Angren industrial area, Uzbekistan. *Environ. Pollut.* **2010**, *158*, 2888–2899. [CrossRef]
41. Sun, Z.; Liu, J.; Zhuo, S.; Chen, Y.; Zhang, Y.; Shen, H.; Yun, X.; Shen, G.; Liu, W.; Zeng, E.Y.; et al. Occurrence and geographic distribution of polycyclic aromatic hydrocarbons in agricultural soils in eastern China. *Environ. Sci. Pollut. Res.* **2017**, *24*, 12168–12175. [CrossRef]
42. Liu, Z.; Liu, D.; Yao, Y. Study on distribution and deposit law of polycyclic aromatic hydrocarbon in coal. *Coal Sci. Technol.* **2010**, *38*, 113–125. (In Chinese with English Abstract) [CrossRef]
43. Niu, Z. Distribution and Environmental Significance of Polycyclic Aromatic Hydrocarbons in Various Coals. Master's Thesis, University of Science and Technology of China, Hefei, China, 2008.
44. Albuquerque, M.; Coutinho, M.; Borrego, C. Long-term monitoring and seasonal analysis of polycyclic aromatic hydrocarbons (PAHs) measured over a decade in the ambient air of Porto, Portugal. *Sci. Total Environ.* **2016**, *543*, 439–448. [CrossRef] [PubMed]

45. Hussain, K.; Rahman, M.; Prakash, A.; Hoque, R.R. Street dust bound PAHs, carbon and heavy metals in Guwahati city—Seasonality, toxicity and sources. *Sustain. Cities Soc.* **2015**, *19*, 17–25. [CrossRef]
46. Li, Y.; Song, N.; Yu, Y.; Yang, Z.; Shen, Z. Characteristics of PAHs in street dust of Beijing and the annual wash-off load using an improved load calculation method. *Sci. Total Environ.* **2017**, *581–582*, 328–336. [CrossRef] [PubMed]
47. Yunker, M.B.; Macdonald, R.W.; Vingarzan, R.; Mitchell, R.H.; Goyette, D.; Sylvestre, S. PAHs in the Fraser River basin: A critical appraisal of PAH ratios as indicators of PAH source and composition. *Org. Geochem.* **2002**, *33*, 489–515. [CrossRef]
48. Budzinski, H.; Jones, I.; Bellocq, J.; Piérard, C.; Garrigues, P. Evaluation of sediment contamination by polycyclic aromatic hydrocarbons in the Gironde estuary. *Mar. Chem.* **1997**, *58*, 85–97. [CrossRef]
49. Pies, C.; Hoffmann, B.; Petrowsky, J.; Yang, Y.; Ternes, T.A.; Hofmann, T. Characterization and source identification of polycyclic aromatic hydrocarbons (PAHs) in river bank soils. *Chemosphere* **2008**, *72*, 1594–1601. [CrossRef]
50. Tobiszewśki, M.; Namieśnik, J. PAH diagnostic ratios for the identification of pollution emission sources. *Environ. Pollut.* **2012**, *162*, 110–119. [CrossRef]
51. USEPA. *USEPA Soil Screening Guidance: User's Guide*, 2nd ed.; Environmental Protection Agency: Washington, DC, USA, 1996. Available online: http://nepis.epa.gov/Exe/ZyPURL.cgi?Dockey=100027WI.txt (accessed on 1 May 2022).
52. USEPA. *Application of the Margin of Exposure (MoE) Approach to Substances in Food that are Genotoxic and Carcinogenic Example: Benzo[a]pyrene and Polycyclic Aromatic Hydrocarbons*; Environmental Protection Agency: Washington, DC, USA, 2010. Available online: https://cfpub.epa.gov/si/si_public_record_report.cfm?dirEngryId=218290 (accessed on 1 May 2022).
53. Nisbet, I.C.T.; LaGoy, P.K. Toxic equivalency factors (TEFs) for polycyclic aromatic hydrocarbons (PAHs). *Regul. Toxicol. Pharmacol.* **1992**, *16*, 290–300. [CrossRef]
54. USEPA. *"Benzo[a]pyrene (BaP)(CASRN 50-32-8)"*; Environmental Protection Agency: Washington, DC, USA, 1994. Available online: http://www.epa.gpv/ncea/iris/subst/0136.htm (accessed on 1 May 2022).
55. USEPA. *Human Health Evaluation Manual, Supplemental Guidance: Update of Standard Default Exposure Factors*; OSWER Directive 9200; Environmental Protection Agency: Washington, DC, USA, 2014; pp. 1–120.
56. National Bureau of Statistics of the People's Republic of China. 2010. Available online: http://data.stats.gov.cn/ (accessed on 1 May 2022).
57. United State Department of Energy. *The Risk Assessment Information System (RAIS)*; U.S. Department of Energy's Oak Ridge Operations Office (ORO): Oak Ridge, TN, USA, 2011. Available online: http://rais.ornl.gov/ (accessed on 1 May 2022).
58. Albanese, S.; Fontaine, B.; Chen, W.; Lima, A.; Cannatelli, C.; Piccolo, A. Polycyclic aromatic hydrocarbons in the soils of a densely populated region and associated human health risks: The Campania Plain (Southern Italy) case study. *Environ. Geochem. Health* **2014**, *37*, 1–20. [CrossRef]
59. Zhang, J.; Qu, C.; Qi, S.; Cao, J.; Zhan, C.; Xing, X.; Xiao, Y.; Zheng, J.; Xiao, W. Polycyclic aromatic hydrocarbons (PAHs) in atmospheric dustfall from the industrial corridor in Hubei Province, Central China. *Environ. Geochem. Health* **2015**, *37*, 891–903. [CrossRef]